

Universality of dispersive spin-resonance mode in superconducting BaFe₂As₂

C. H. Lee,^{1,2} P. Steffens,³ N. Qureshi,⁴ M. Nakajima,^{1,2} K. Kihou,^{1,2} A. Iyo,^{1,2} H. Eisaki,^{1,2} and M. Braden⁴

¹National Institute of Advanced Industrial Science and Technology (AIST), Tsukuba, Ibaraki 305-8568, Japan

²Transformative Research-Project on Iron Pnictides (TRIP), JST, Chiyoda, Tokyo 102-0075, Japan

³Institut Laue Langevin, 6 Rue Jules Horowitz BP 156, F-38042 Grenoble CEDEX 9, France

⁴II. Physikalisches Institut, Universität zu Köln, Zùlpicher Str. 77, D-50937 Köln, Germany

Spin fluctuations in superconducting BaFe₂(As_{1-x}P_x)₂ (x=0.34, $T_c = 29.5$ K) are studied using inelastic neutron scattering. Well-defined commensurate magnetic signals are observed at $(\pi,0)$, which is consistent with the nesting vector of the Fermi surface. Antiferromagnetic (AFM) spin fluctuations in the normal state exhibit a three-dimensional character reminiscent of the AFM order in nondoped BaFe₂As₂. A clear spin gap is observed in the superconducting phase forming a peak whose energy is significantly dispersed along the c-axis. The bandwidth of dispersion becomes larger with approaching the AFM ordered phase universally in all superconducting BaFe₂As₂, indicating that the dispersive feature is attributed to three-dimensional AFM correlations. The results suggest a strong relationship between the magnetism and superconductivity.

PACS numbers: 74.70.Xa, 75.40.Gb, 78.70.Nx

Magnetism is considered to play a crucial role on the appearance of superconductivity in iron-based superconductors [1]. To verify this assumption, the relationship between superconductivity and spin fluctuations has been studied intensively. Carrier-doped superconducting AFe₂As₂ (A = Ba, Sr and Ca) is one of the systems which have been well studied using inelastic neutron scattering [2–18] due to the availability of sizable single crystals. Spin fluctuations are observed around $(\pi,0)$ [(0.5,0.5,L) in tetragonal notation] in the system, where their peak positions are determined by the topology of the Fermi surface (FS) [2–5]. They exhibit a gap structure in the superconducting phase with remarkable enhancement of the magnetic signal at a specific energy [5–18].

The interpretation of the enhancement depends on the superconducting gap symmetry. For a s_{\pm} -wave gap, the enhancement is argued to be a spin resonance [19, 20]. In contrast, for a s_{++} -wave gap, it is formed due to the absence of inelastic quasiparticle scattering just on the gap [21, 22]. Thus, it is essential to clarify the origin of the intensity enhancement to determine the superconducting gap symmetry. In this paper, we refer to the intensity enhancement as resonance for convenience, although the interpretation of the enhancement is still controversial.

The resonance characteristics of iron-based superconductors are complicated. In Co- and Ni-doped BaFe₂As₂, they depend on the L value [5–9] and exhibit a pronounced spin-space anisotropy [13–15]. The resonance energies are larger for even values of L than for odd values. Polarized neutron scattering measurements in optimum Co-doped BaFe₂As₂ have revealed an additional sharp peak at an energy of $1.8k_B T_c$, which is considerably below the resonance observed in unpolarized neutron-scattering measurements [13]. Here, k_B denotes the Boltzmann constant. The origin of the anisotropies is still unexplained although clear understanding of the resonance is important for clarifying the mechanism of

Cooper pair formation. Therefore, in the present paper, we try to reveal the origin in particular of the dependence on L .

Two different interpretations have been proposed to explain the dispersive feature of the resonance. One has attributed it to the c-axis dependence of the superconducting gap under the assumption that the resonance energy is associated with the superconducting gap value [6, 7]. The other has argued that it arises from interlayer spin correlations based on the random-phase approximation (RPA) calculations where the resonance results from the formation of spin excitons [9, 23]. Stronger spin correlation can cause lower resonance energies in this model.

To solve the problem, it is efficient to compare the resonance in samples whose superconductivity is induced by different methods resulting in nonequivalent superconducting gap anisotropy. For this purpose, AFe₂As₂ is a suitable system because superconductivity can be controlled in several ways, namely: electron [24] or hole doping [25], external pressure [26], and chemical pressure induced by P-doping at the As site [27]. Although intensive studies on spin fluctuations have been carried out by inelastic neutron scattering using single crystals of carrier-doped superconducting AFe₂As₂, studies on samples whose superconductivity is induced by other methods have been restricted to powder samples [28]. We therefore conducted inelastic neutron scattering measurements on single crystals of superconducting BaFe₂(As,P)₂, where the superconductivity occurs without carrier doping. We found that the resonance energy depends strongly on L , indicating the universality of its dispersive feature in the superconducting phase.

Single crystals of BaFe₂(As_{1-x}P_x)₂ were grown by the self-flux method, which is described in detail elsewhere [29]. Approximately 260 tabular-shaped single crystals (~ 0.06 cm³) taken from the same batch were co-aligned on thin Al sample holders for inelastic neutron scat-

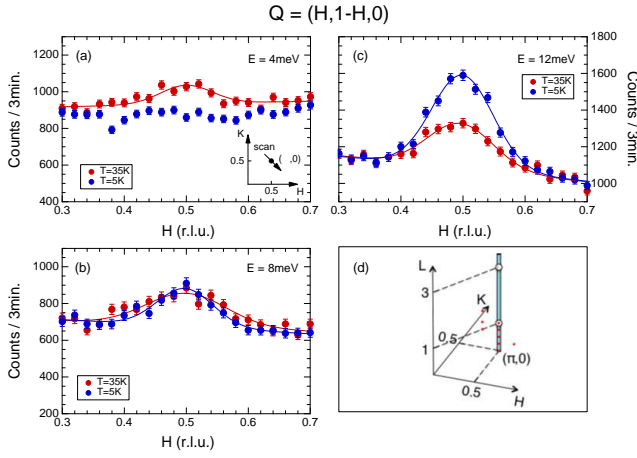


FIG. 1. (a)-(c) Constant-energy scans of $\text{BaFe}_2(\text{As,P})_2$ in the $(H,K,0)$ zone above and below T_c for (a) $E = 4$ meV, (b) $E = 8$ meV, and (c) $E = 12$ meV. The scan trajectory is indicated by the arrow in panel (a). Solid lines indicate Gaussian fits. (d) Schematic illustrations of magnetic peak positions forming a rod structure in $\text{BaFe}_2(\text{As,P})_2$. Open circles at $(0.5, 0.5, L)$ with odd L describe the peak positions of AFM long-range order in nondoped BaFe_2As_2 . Dots describe measured positions in constant- \mathbf{Q} scans shown in Fig. 3.

tering measurements. The total mosaic spreads of the co-aligned samples had full widths at half maximum of $\sim 2.5^\circ$ and $\sim 3.5^\circ$ in the (H,H,L) and $(H,K,0)$ scattering planes used in our experiment, respectively. The T_c of the single crystals was determined to be 29.5 K from the temperature dependence of the zero-field-cooled magnetization using a SQUID magnetometer (Quantum Design MPMS) under a magnetic field of 10 Oe parallel to the c -axis. The P content in the single crystals was determined to be $x = 0.34$ based on the T_c value and c -axis lattice parameters obtained from X-ray diffraction [29].

Inelastic neutron scattering measurements were conducted using the triple-axis spectrometer IN8 at the Institute Laue-Langevin in Grenoble, France. The final neutron energy was fixed at $E_f = 14.7$ meV by using double-focusing pyrolytic graphite (PG) crystals as a monochromator and analyzer. No collimator was used to maximize the intensity. A PG filter was inserted to remove higher-order neutrons. A He cryostat was used to cool the samples down to 5 K.

Figures 1(a-c) show \mathbf{q} scans measured in the $[1,-1,0]$ direction of the $(H,K,0)$ zone at $T = 35$ and 5 K. Well-defined commensurate peaks are observed at $\mathbf{Q} = (0.5, 0.5, 0)$ with a spin gap opening below T_c . At $E = 4$ meV, the magnetic intensity vanishes at $T = 5$ K due to the spin gap. At $E = 8$ meV, the peak intensity remains constant upon cooling, whereas it increases remarkably at $E = 12$ meV.

Commensurate peaks are also observed in the \mathbf{q} -spectra measured in the $[1,1,0]$ direction of the (H,H,L) zone for integer and non-integer L values (Fig. 2). These

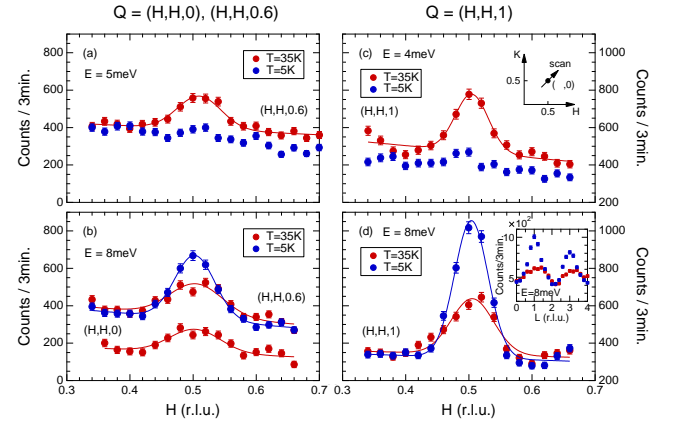


FIG. 2. Constant-energy scans of $\text{BaFe}_2(\text{As,P})_2$ in the (H,H,L) zone above and below T_c . (a,b) \mathbf{q} scans at $L = 0$ and 0.6 for (a) $E = 5$ meV and (b) $E = 8$ meV. The spectrum at $L = 0$ is shifted down by 200 counts to facilitate viewing. (c,d) \mathbf{q} scans at $L = 1$ for (c) $E = 4$ meV and (d) $E = 8$ meV. The scan trajectory is indicated by the arrow in panel (c). Solid lines indicate Gaussian fits. The inset in panel (d) shows the L dependence of the magnetic peak intensities above and below T_c for $E = 8$ meV.

commensurate peaks indicate that magnetic peaks form a rod structure along the c -axis at $\mathbf{Q} = (0.5, 0.5, L)$ [Fig. 1(d)]. Spin gaps are also observed at $L = 0.6$ and 1 below T_c [Figs. 2(a,c)]. An enhancement of the peak intensity below T_c is observed at $E = 8$ meV for $L = 0.6$ and 1 [Fig. 2(b,d)]. The peak intensities strongly depend on the L value at $E = 8$ meV for both $T = 5$ and 35 K [Figs. 2(b,d)]. They exhibit maximum intensity at odd values of L [inset of Fig. 2(d)], where the long-range antiferromagnetic (AFM) order in nondoped BaFe_2As_2 forms magnetic Bragg peaks in elastic scattering.

The energy dependence of the magnetic scattering at $T = 35$ and 5 K was measured at several L values with the background determined at the sides of the magnetic rod [Figs. 3 (a,c)]. The dynamical magnetic susceptibility $\chi''(\mathbf{q}, \omega)$ was obtained by multiplying the net intensity by $[1 - \exp(-\hbar\omega/k_B T)]$ after correcting for higher-order components in the incident beam monitor [30] [Figs. 3 (b,d)]. $\chi''(\mathbf{q}, \omega)$ at $T = 35$ K for $L = 0, 0.25$ and 0.5 increases monotonically with increasing energy and tends to saturate, as is usually observed in correlated spin systems without magnetic long-range ordering. Additional signals were observed below $E = 9$ meV at $L = 0.75$ and 1, in agreement with the L dependence of the intensity at $E = 8$ meV shown in the inset of Fig. 2(d). Magnetic correlations in $\text{BaFe}_2(\text{As}_{0.66}\text{P}_{0.34})_2$ possess hence a three-dimensional character reflecting the fully three-dimensional AFM order observed in nondoped BaFe_2As_2 . We verified that there is no detectable elastic magnetic signal appearing at $\mathbf{Q} = (0.5, 0.5, 1)$ above $T = 5$ K, confirming that there is no sizeable static AFM order in $\text{BaFe}_2(\text{As}_{0.66}\text{P}_{0.34})_2$.

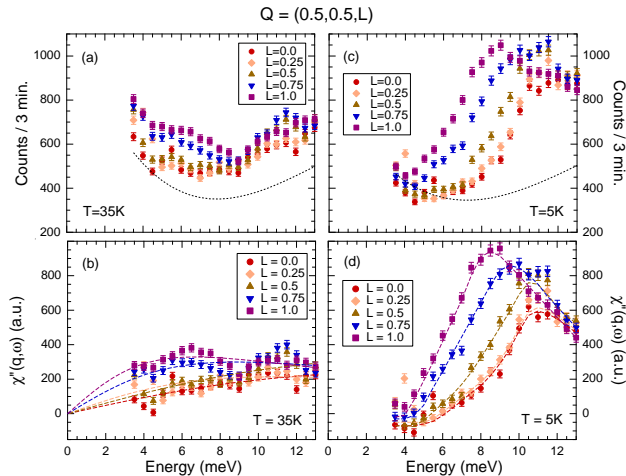


FIG. 3. (a,c) Constant- \mathbf{Q} scans at $\mathbf{Q} = (0.5, 0.5, L)$ for several L values (a) above and (c) below T_c . Dotted lines describe the background determined by averaging the background at $\mathbf{Q} = (0.38, 0.38, 1)$, $(0.38, 0.38, 1.25)$, $(0.38, 0.38, 1.65)$, and $(0.62, 0.62, 0)$. Measured \mathbf{Q} positions are described in Fig. 1 (d). (b,d) Energy spectra of $\chi''(\mathbf{q}, \omega)$ (b) above and (d) below T_c . These were obtained by subtracting the background and by correcting for the monitor higher-order contamination and for the Bose factor. The dashed lines in panel (b) are fits obtained using Eq. (1), and those in panel (d) are guides to the eye.

The energy dependence of $\chi''(\mathbf{q}, \omega)$ in the normal state was fitted using a phenomenological function applicable to correlated spin systems in Fermi liquids without magnetic long-range ordering,

$$\chi''(\mathbf{q}, \omega) = \chi_0 \frac{\Gamma \hbar \omega}{\Gamma^2 + (\hbar \omega)^2}, \quad (1)$$

where χ_0 represents the strength of the AFM correlation, and Γ is a damping constant. Fitting results are shown by the solid lines in Fig. 3 (b). The evaluated Γ decreases from 20.5 ± 7.5 meV to 6.5 ± 1 meV when L varies from 0 to 1. The fitted lines at $L = 0, 0.25$ and 0.5 reproduce the data reasonably well, whereas those at $L = 0.75$ and 1 reproduce the data only moderately well because the additional feature below $E = 9$ meV cannot be described appropriately. Thus, the data at $L = 0.75$ and 1 seem to be beyond the framework of equation (1). This could be because the sample is close to AFM long-range ordering.

$\chi''(\mathbf{q}, \omega)$ in the superconducting state at $T = 5$ K exhibits apparent spin gap structures at all values of L with a clear peak referred to as resonance [Fig. 3 (d)]. The resonance energy and intensity strongly depend on L . The additional low-energy peak observed by polarized inelastic neutron scattering in Co-doped BaFe_2As_2 below T_c [13] can also be included in the present $\chi''(\mathbf{q}, \omega)$. By analogy, the expected peak energy would be $E = 4.6$ meV. In fact, subtle humps might be seen in the low en-

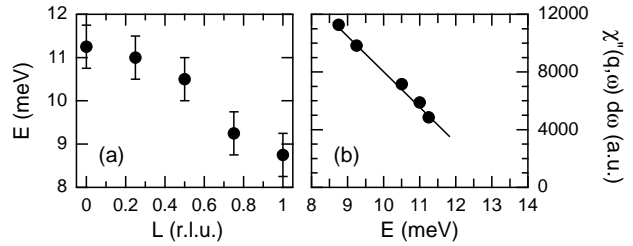


FIG. 4. (a) L dispersion of resonance energy defined as the intensity maximum in the energy spectra shown in Fig. 3(d). (b) Resonance energy dependences of energy-integrated $\chi''(\mathbf{q}, \omega)$ over $E = 3.5$ to 13 meV at $T = 5$ K.

ergy region, although the energy is slightly higher than the expected one. Our experiment is, however, unable to fully separate the humps from the main peak without using polarized neutrons. In the following, we will focus on the main response whose intensity maxima can be unambiguously determined due to its sufficiently high intensity, despite the overlap with the low-energy shoulders.

Figure. 4 (a) shows the dispersion of the resonance. The observed resonance energies correspond to $2\Delta/k_B T_c = 3.4 - 4.4$. The energy is lower for odd values of L , where magnetic signals of three-dimensional character are found in the normal state. The energy-integrated $\chi''(\mathbf{q}, \omega)$ up to $E = 13$ meV at $T = 5$ K decreases linearly with increasing resonance energy [Fig. 4 (b)]. The linear relationship is qualitatively consistent with the RPA calculations where the resonance is interpreted as the formation of spin excitons [5, 23, 31]. It is predicted that the energy of resonance decreases and intensity increases with increasing an exchange constant. Because the calculations were applied to d-wave superconductors, they should be extended to deal with the s-wave gap to explain the present results. The required assumption is that the onset of the particle-hole continuum should be independent of L . According to angle-resolved photoemission spectroscopy, superconducting gaps of $\text{BaFe}_2(\text{As}_{1-x}\text{P}_x)_2$ depend on the c-axis wave vector and exhibit a nodal gap structure at the Z-point on the outmost hole FS [32]. However, the nodal gap cannot directly be sensed in our experiment. First the size and the orbital character do not match with the counterpart electron FS. In addition, the inelastic neutron scattering experiment integrates all processes between the nested FS's which are gapped in the superconducting state. In particular, it averages the distribution of gap values along the c-axis. Isotropic superconducting gaps along the c-axis are, thus, not required.

The doping dependence of the bandwidth ($E_{L=\text{even}} - E_{L=\text{odd}}$) of the resonance dispersion along L is analyzed

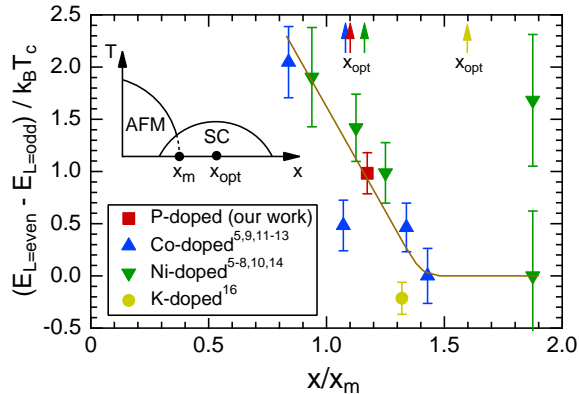


FIG. 5. Doping dependence of the bandwidth ($E_{L=\text{even}} - E_{L=\text{odd}}$) of the resonance dispersion along L for various iron-based superconductors [5–14, 16]. Energies are normalized by $k_B T_c$ and the doping levels are normalized by the levels where AFM ordering disappears (x_m). The x_m values are assumed to be 29 %, 5.6 %, 4 %, and 25 % for P-, Co-, Ni-, and K-doped samples, respectively. The optimum doping level (x_{opt}) is depicted by arrows. The solid line is a guide to the eye.

for various iron-based superconductors in Fig. 5. For comparison, energies are normalized by $k_B T_c$, and the doping levels are normalized by compositions where AFM ordering disappears (x_m). Values of x_m were determined from each phase diagram by extrapolating their Néel temperatures [29, 33–37]. In fact, the two samples which have values of x/x_m less than 1 exhibit AFM long-range ordering [7, 9], whereas the others do not, which justifies the present estimation of x_m . Although the estimation is rough, it is sufficient to figure out the overall picture. As shown in Fig. 5, the normalized bandwidth increases with decreasing doping level following a universal curve. This suggests that the energy dispersion has a common origin and that it is related to the AFM state. The dispersion has not been found in K-doped samples yet, which is likely due to too high doping of the samples used in inelastic neutron scattering experiments.

Based on the results, the carrier concentration cannot be an essential factor for the L dispersion of the resonance as there is no electron doping in P-doped samples. Also details of the FS nesting can be discarded, because the topology of FS should be different between electron and P-doped samples. Either the nodal or anisotropic structure of the superconducting gap should also be irrelevant because samples with optimum electron doping exhibit a full gap [38], whereas optimum P-doped samples exhibit a nodal gap [39], although they show similar L dispersion. The dispersion can rather be associated with three-dimensional AFM correlations, as it clearly depends on the doping levels normalized by x_m . A larger dispersion can be caused by a larger three-dimensional

AFM correlation. In fact, the present P-doped sample shows short-range three-dimensional AFM correlation in the normal state and the resonance energy is low at a q -position where the AFM correlation is strong. Electron-underdoped superconducting samples which show the largest dispersion even exhibit three-dimensional AFM ordering [7, 9]. These results provide evidence that the L dispersion is related to the three-dimensional character of AFM correlations consistent with the RPA calculations, suggesting a strong relationship between magnetism and superconductivity. The resonance can be explained by the spin exciton model, which supports the s_{\pm} -wave gap.

In summary, well-defined commensurate spin fluctuations have been observed at $(\pi, 0)$ in optimum doped $\text{BaFe}_2(\text{As}_{1-x}\text{P}_x)_2$. A clear spin gap forms in the superconducting phase with resonance energies dispersing along the c direction. A lower resonance energy is observed at $(0.5, 0.5, L = \text{odd})$. The dispersive feature of the resonance can be attributed to the three-dimensional character of AFM correlations and thus to the neighborhood of the static AFM ordered phase, suggesting a strong relationship between magnetism and superconductivity.

We wish to thank T. Tohyama and T. Yoshida for valuable discussions. This study was supported by a Grant-in-Aid for Scientific Research B (No. 24340090) from the Japan Society for the Promotion of Science and by the Deutsche Forschungsgemeinschaft through SFB608.

-
- [1] P. J. Hirschfeld, M. M. Korshunov, and I. I. Mazin, Rep. Prog. Phys. **74**, 124508 (2011).
 - [2] D. K. Pratt, M. G. Kim, A. Kreyssig, Y. B. Lee, G. S. Tucker, A. Thaler, W. Tian, J. L. Zarestky, S. L. Budko, P. C. Canfield, B. N. Harmon, A. I. Goldman, and R. J. McQueeney, Phys. Rev. Lett. **106**, 257001 (2011).
 - [3] H. Luo, Z. Yamani, Y. Chen, X. Lu, M. Wang, S. Li, T. A. Maier, S. Danilkin, D. T. Adroja, and P. Dai, Phys. Rev. B **86**, 024508 (2012).
 - [4] C. H. Lee, K. Kihou, H. Kawano-Furukawa, T. Saito, A. Iyo, H. Eisaki, H. Fukazawa, Y. Kohori, K. Suzuki, H. Usui, K. Kuroki, and K. Yamada, Phys. Rev. Lett. **106**, 067003 (2011).
 - [5] J. T. Park, D. S. Inosov, A. Yaresko, S. Graser, D. L. Sun, Ph. Bourges, Y. Sidis, Yuan Li, J.-H. Kim, D. Haug, A. Ivanov, K. Hradil, A. Schneidewind, P. Link, E. Faulhaber, I. Glavatsky, C. T. Lin, B. Keimer, and V. Hinkov, Phys. Rev. B **82**, 134503 (2010).
 - [6] S. Chi, A. Schneidewind, J. Zhao, L. W. Harriger, L. Li, Y. Luo, G. Cao, Z. Xu, M. Loewenhaupt, J. Hu, and P. Dai, Phys. Rev. Lett. **102**, 107006 (2009).
 - [7] M. Wang, H. Luo, J. Zhao, C. Zhang, M. Wang, K. Marty, S. Chi, J. W. Lynn, A. Schneidewind, S. Li, and P. Dai, Phys. Rev. B **81**, 174524 (2010).
 - [8] S. Li, Y. Chen, S. Chang, J. W. Lynn, L. Li, Y. Luo, G. Cao, Z. Xu, and P. Dai, Phys. Rev. B **79**, 174527 (2009).
 - [9] D. K. Pratt, A. Kreyssig, S. Nandi, N. Ni, A. Thaler, M.

- D. Lumsden, W. Tian, J. L. Zarestky, S. L. Budko, P. C. Canfield, A. I. Goldman, and R. J. McQueeney, *Phys. Rev. B* **81**, 140510(R) (2010).
- [10] M. Liu, C. Lester, J. Kulda, X. Lu, H. Luo, M. Wang, S. M. Hayden, and P. Dai, *Phys. Rev. B* **85**, 214516 (2012).
- [11] D. S. Inosov, J. T. Park, P. Bourges, D. L. Sun, Y. Sidis, A. Schneidewind, K. Hradil, D. Haug, C. T. Lin, B. Keimer, and V. Hinkov, *Nat. Phys.* **6**, 178 (2010).
- [12] M. D. Lumsden, A. D. Christianson, D. Parshall, M. B. Stone, S. E. Nagler, G. J. MacDougall, H. A. Mook, K. Lokshin, T. Egami, D. L. Abernathy, E. A. Goremychkin, R. Osborn, M. A. McGuire, A. S. Sefat, R. Jin, B. C. Sales, and D. Mandrus, *Phys. Rev. Lett.* **102**, 107005 (2009).
- [13] P. Steffens, C. H. Lee, N. Qureshi, K. Kihou, A. Iyo, H. Eisaki, and M. Braden, *Phys. Rev. Lett.* **110**, 137001 (2013).
- [14] O. J. Lipscombe, L. W. Harriger, P. G. Freeman, M. Enderle, C. Zhang, M. Wang, T. Egami, J. Hu, T. Xiang, M. R. Norman, and P. Dai, *Phys. Rev. B* **82**, 064515 (2010).
- [15] C. Zhang, M. Liu, Y. Su, L. P. Regnault, M. Wang, G. Tan, Th. Brückel, T. Egami, and P. Dai, *Phys. Rev. B* **87**, 081101(R) (2013).
- [16] C. Zhang, M. Wang, H. Luo, M. Wang, M. Liu, J. Zhao, D. L. Abernathy, T. A. Maier, K. Marty, M. D. Lumsden, S. Chi, S. Chang, J. A. Rodriguez-Rivera, J. W. Lynn, T. Xiang, J. Hu, and P. Dai, *Sci. Rep.* **1**, 115 (2011).
- [17] A. D. Christianson, E. A. Goremychkin, R. Osborn, S. Rosenkranz, M. D. Lumsden, C. D. Malliakas, I. S. Todorov, H. Claus, D. Y. Chung, M. G. Kanatzidis, R. I. Bewley, and T. Guidi, *Nature* **456**, 930 (2008).
- [18] A. D. Christianson, M. D. Lumsden, S. E. Nagler, G. J. MacDougall, M. A. McGuire, A. S. Sefat, R. Jin, B. C. Sales, and D. Mandrus, *Phys. Rev. Lett.* **103**, 087002 (2009).
- [19] I. I. Mazin, D. J. Singh, M. D. Johannes, and M. H. Du, *Phys. Rev. Lett.* **101**, 057003 (2008).
- [20] K. Kuroki, S. Onari, R. Arita, H. Usui, Y. Tanaka, H. Kontani, and H. Aoki, *Phys. Rev. Lett.* **101**, 087004 (2008).
- [21] S. Onari, H. Kontani, and M. Sato, *Phys. Rev. B* **81**, 060504(R) (2010).
- [22] S. Onari, and H. Kontani, *Phys. Rev. B* **84**, 144518 (2011).
- [23] M. Eschrig, *Adv. Phys.* **55**, 47 (2006).
- [24] A. S. Sefat, R. Jin, M. A. McGuire, B. C. Sales, D. J. Singh, and D. Mandrus, *Phys. Rev. Lett.* **101**, 117004 (2008).
- [25] M. Rotter, M. Tegel, and D. Johrendt, *Phys. Rev. Lett.* **101**, 107006 (2008).
- [26] P. L. Alireza, Y. T. C. Ko, J. Gillett, C. M. Petrone, J. M. Cole, G. G. Lonzarich, and S. E. Sebastian, *J. Phys.: Condens. Matter* **21**, 012208 (2009).
- [27] S. Jiang, H. Xing, G. Xuan, C. Wang, Z. Ren, C. Feng, J. Dai, Z. Xu, and G. Cao, *J. Phys.: Condens. Matter* **21**, 382203 (2009).
- [28] M. Ishikado, Y. Nagai, K. Kodama, R. Kajimoto, M. Nakamura, Y. Inamura, S. Wakimoto, H. Nakamura, M. Machida, K. Suzuki, H. Usui, K. Kuroki, A. Iyo, H. Eisaki, M. Arai, and S. Shamoto, *Phys. Rev. B* **84**, 144517 (2011).
- [29] M. Nakajima, S. Uchida, K. Kihou, C. H. Lee, A. Iyo, and H. Eisaki, *J. Phys. Soc. Jpn.* **81**, 104710 (2012).
- [30] G. Shirane, S. M. Shapiro, and J. M. Tranquada, *Neutron Scattering with a Triple-Axis Spectrometer*, (Cambridge University Press, 2002), p. 117.
- [31] A. J. Millis, and H. Monien, *Phys. Rev. B* **54**, 16172 (1996).
- [32] Y. Zhang, Z. R. Ye, Q. Q. Ge, F. Chen, Juan Jiang, M. Xu, B. P. Xie, and D. L. Feng, *Nat. Phys.* **8**, 371 (2012).
- [33] S. Kasahara, H. J. Shi, K. Hashimoto, S. Tonegawa, Y. Mizukami, T. Shibauchi, K. Sugimoto, T. Fukuda, T. Terashima, Andriy H. Nevidomskyy, and Y. Matsuda, *Nature* **486**, 382 (2012).
- [34] J.-H. Chu, J. G. Analytis, Chris Kucharczyk, and Ian R. Fisher, *Phys. Rev. B* **79**, 014506 (2009).
- [35] P. C. Canfield, S. L. Budko, N. Ni, J. Q. Yan, and A. Kracher, *Phys. Rev. B* **80**, 060501(R) (2009).
- [36] S. Avci, O. Chmaissem, D. Y. Chung, S. Rosenkranz, E. A. Goremychkin, J. P. Castellán, I. S. Todorov, J. A. Schlueter, H. Claus, A. Daoud-Aladine, D. D. Khalyavin, M. G. Kanatzidis, and R. Osborn, *Phys. Rev. B* **85**, 184507 (2012).
- [37] M. Rotter, M. Pangerl, M. Tegel, and D. Johrendt: *Angew. Chem. Int. Ed.* **47** (2008) 7949.
- [38] J.-Ph. Reid, M. A. Tanatar, X. G. Luo, H. Shakeripour, N. Doiron-Leyraud, N. Ni, S. L. Budko, P. C. Canfield, R. Prozorov, and Louis Taillefer, *Phys. Rev. B* **82**, 064501 (2010).
- [39] K. Hashimoto, M. Yamashita, S. Kasahara, Y. Senshu, N. Nakata, S. Tonegawa, K. Ikada, A. Serafin, A. Carrington, T. Terashima, H. Ikeda, T. Shibauchi, and Y. Matsuda, *Phys. Rev. B* **81**, 220501(R) (2010).